Mem. S.A.It. Suppl. Vol. 19, 222

Memorie della
Supplementi

Dark Matter in Elliptical Galaxies

N. R. Napolitano

Istituto Nazionale di Astrofisica – Osservatorio Astronomico di Capodimonte, Salita Moiariello 16, 80131 Napoli, Italy e-mail: napolita@na.astro.it

Abstract. Latest evidences from separated analysis of the dark matter (DM) content of central and halo regions of elliptical galaxies show that these systems lie fairly within the ΛCDM framework. Their DM properties show a large scatter around typical scaling relations of dark haloes, but this seems to be a consequence of the complicated variety of the physical processes acting during their evolution, rather than the intrinsic properties of their parent haloes. Hence, it seems currently important to carefully account for the baryon physics, including the stellar population properties, and its role in shaping the DM distribution around galaxies. This would possibly explain the large variance of the inferred density parameters which leave still rooms for different families of DM density profiles (from cuspy to cored profiles).

Key words. Galaxies: Ellipticals – Galaxies: Kinematics and Dynamics – Galaxies: Structure – Dark matter

1. Introduction

The ΛCDM cosmological model has provided a compelling picture for the formation and evolution of structure the universe. In particular, galaxies form as gas cools to stars at the bottom of the potential wells of DM halos (White & Rees 1978) which are found to evolve through hierarchical assembly in N-body (collisionless) simulations (Thomas & Couchman 1992, Navarro et al. 1997, NFW hereafter). In these simulations, dark haloes (DHs) are found to have a universal density distribution (independent of the total virial mass) characterized by a steep central cusp (NFW,Moore et al. 1999).

The observational tests of these predictions still show a number of discrepancies at galaxy and cluster scales, which need to be clarified. For instance, steep central cusps seem incompatible with many observations of late-type galaxies (de Blok, Bosma, & McGaugh 2003; Gentile et al. 2004), which seem to favor DM halos with a lower concentration. It remains to be seen whether this divergence can be traced to observational problems rather than to oversimplified predictions of the halo properties, or to a failure of the ΛCDM paradigm.
Given the long-standing DM puzzles in disk galaxies, it has become more and more important to have a deeper insight on the mass content of the other big galaxy family, that of the early-type galaxies (ETGs), i.e. ellipticals and S0s. Since these objects are usually free of cold gas and have their stars moving in random directions, their kinematics is more difficult to sample than in disk galaxies and their dynamics harder to model, a fact that adds uncertainties in the mass estimates of these galaxies and

Send offprint requests to: N.R. Napolitano

consequently on the actual "weight of the dark component".

2. The central regions of ETGs

In the last decades, the analysis of DM content in the central regions of ETGs has been improved with multiple observational campaigns: fiber aperture and long-slit spectroscopy at multiple position angles have been standard technique to derive information on the galaxy central regions (out to $2\,R_{\rm e}$, the radius that encircles half of the total light of the galaxy – Bender et al. 1994, Statler & Smecker-Hane 1999), nowadays complemented with sophisticated integral field spectrographs (e.g., SAURON@WHT, VIMOS-IFU@VLT) which are producing complete 2D kinematical maps of galaxies (e.g., Emsellem et al. 2007).

There are increasing evidences pointing to a central DM fraction which is an increasing function of luminosity, stellar mass or size (Cappellari et al. 2006, Hyde & Bernardi 2009, Tortora et al. 2009, T+09 hereafter, Auger et al. 2010). Because of the tight positive correlation between $R_{\rm e}$ and stellar mass or luminosity, the strong increasing trend of DM fraction inside the $R_{\rm e}$ seems to be due to the larger effective radii enclosing a bigger portion of the DM halo, rather than be driven by the mass. This can be interpreted in the hierarchical scenario of galaxy formation in the sense that larger and more massive galaxies appear to have experienced more merging events when compared with smaller and less massive ones. Another way to test the ΛCDM is to compare the galaxy scaling relations over large galaxy samples with predictions of modeled multi-component (e.g. Sérsic (1968) spheroid + NFW halo) galaxies fully reproducing the ΛCDM expectations, to see whether observations match the theory predictions. This is shown, e.g., in Fig. 1 (from Napolitano, Romanowsky & Tortora 2010, NRT10 hereafter) where the average DM density within 1 $R_{\rm e}$ is compared with different model predictions. This result is particularly important because the slope of the $\log\rho - \log R_{\rm e}$ relation ($\sim$ 1.8) is compatible with a cuspy contracted halo.

Even more interesting is the evidence of a strong inverse correlation existing between the central DM fraction and the formation epoch of stars in the ETGs, with younger galaxies having a larger amount of DM in their centers (NRT10, Tortora et al. 2010). The main driver of such a correlation is the inverse correlation between the size and galaxy age, explained within the hierarchical paradigm by some recent semianalytical simulations (Khochfar & Silk 2006) although even adiabatic contraction (AC) or a "differential" initial mass function might have played a role (NRT10). The same effects would be caused by a variation of the IMF with Age: if younger galaxies have a higher-mass IMF (e.g. a Salpeter 1955 IMF), i.e. they have more stellar mass for a given luminosity, then the higher observed dynamical M/L are not due to the excess of DM but to higher stellar mass, thus their DM fraction is overestimated with respect to older systems having a lower-mass IMF (e.g. Chabrier 2001), thus producing a spurious trend with Age. Finally, the variation of the DM fraction in galaxies can be the reflection of a global DM fraction varying with mass (Napolitano et al. 2005, N+05 hereafter) due to a variation of efficiency, $\epsilon_{\rm SF}$, in the star formation with galaxy mass (Benson et al. 2000; van den Bosch et al. 2007; Conroy & Wechsler 2009)[1].

3. The outer regions of ETGs

Outside $\sim$ 1–2 $R_{\rm e}$, the decreasing surface brightness makes kinematics measurements very difficult (e.g. Halliday et al. 2001; Corsini et al. 2008), and other techniques allow to investigate the DM content of these systems.

X-ray emission from the hot gas has allowed the identification of dark halos in a few individual Es (e.g., Paolillo et al. 2003, Humphrey et al. 2006, Pellegrini et al. 2007). Studies of small galaxy samples are contradictory about their consistency with LCDM: the halo concentrations appear to be too low

[1] If one defines the efficiency of the conversion of the gas into stars, such that $\epsilon_{\rm SF} \sim 1/\Omega_{\rm bar} M_*/M_{\rm vir}$ (M_* and $M_{\rm vir}$ being the stellar and virial mass respectively and $\Omega_{\rm bar}$ is the baryonic density parameter), it is easy to connect the $f_{\rm DM}$ with $\epsilon_{\rm SF}$ by the equation $f_{\rm DM} =\sim 1 - \Omega_{\rm bar}\,\epsilon_{\rm SF}$.

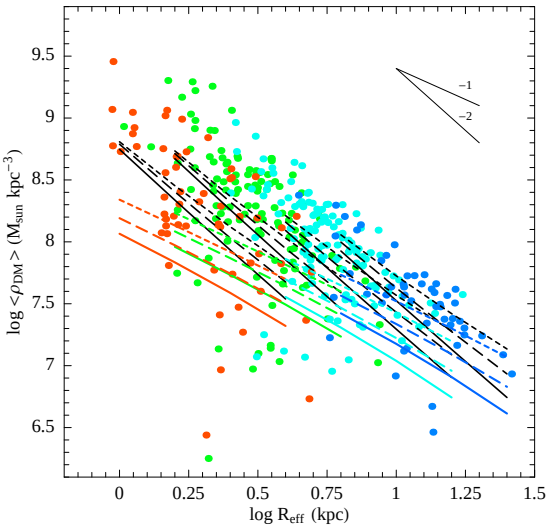

Fig. 1. Relation between DM density within 1 R_e and the R_e value for ETGs in different increasing mass bin from red to blue. The ΛCDM toy model curves are with no AC (colored) and AC (black for G+04) with ϵ_{SF} = 0.05 (dotted), 0.2 (dashed), 0.7 (continuous).

(Fukazawa et al. 2006), or they are normal-to-high (Humphrey et al. 2006). However, the X-ray technique has the limitation that it can apply only to very massive systems, where the hot gas is dense enough to be observed, while for ETGs of average luminosity ($\sim L^* = 2 \times 10^{10} L_\odot$) the low X-ray gas fluxes can make them observationally expensive, and in many cases the gas is in a wind-state far from hydrostatic equilibrium (Pellegrini & Ciotti 2006), such that for galaxies fainter than $M_B \sim -20$, the technique becomes highly un-practicable. Thus, mass studies using X-ray emission are biassed toward massive, group or cluster-central galaxies, while ordinary ETGs are much more difficult to probe (see Paolillo et al. 2003,O'Sullivan & Ponman 2004, Pellegrini et al. 2007).

Globular clusters have classically been used as mass tracers in the haloes of "bright" galaxies, but the kinematical samples in "ordinary" ETGs have so far been too small for strong constraints (e.g. Puzia et al. 2004; Bergond et al. 2006).

Hence it is not surprising that there is no unbiassed, systematic survey of the detailed DM properties of ETGs, comparable to what is available for late-types (Persic et al. 1996).

4. Dark matter distribution with Planetary Nebulae

Planetary nebulae (PNe), are the only probes of the stellar kinematics in ETG haloes: their bright 5007Å OIII emission line can be isolated by the faint galaxy background through contrast ON/OFF band techniques and their velocity measured with individual spectroscopy follow-up(e.g. Ciardullo et al. 1993; Arnaboldi et al. 1998; Napolitano et al. 2002; Peng et al. 2004).

Un the later years, the PN kinematical mapping technique has been made more efficient with Planetary Nebula Spectrograph (PN.S; Douglas et al. 2002), the first custom-designed instrument for galaxy kinematics with PNe. The PN.S has begun producing large kinematical samples of PNe in a variety of galaxy types (Merrett et al. 2006; Romanowsky et al. 2003, R+03 hereafter, Douglas et al. 2007; Noordermeer et al. 2008, Coccato et al. 2009, C+09).

In particular, PNe positions and radial velocities for 9 early-type galaxies have been used to derive two-dimensional velocity and velocity dispersion fields (C+09). The emerging picture is that 1) PNe number density distribution and kinematics (rotation and dispersion) follow the stellar surface brightness and line-of-sight kinematics respectively; 2) the mean rms velocity profiles fall into two groups: slowly decreasing profiles and steeply falling profiles; 3) many objects are more rotationally dominated at large radii than in their central parts; and 4) the halo kinematics are correlated with other galaxy properties (total B-band and X-ray luminosity, isophotal shape, total stellar mass, V/σ), with a clear separation between fast and slow rotators.

This dichotomy of the dispersion profiles may reflect, in principle, different DM properties. In particular the pseudo-keplerian decline in the velocity dispersion profile of "ordinary" elliptical, seemed more suggestive of

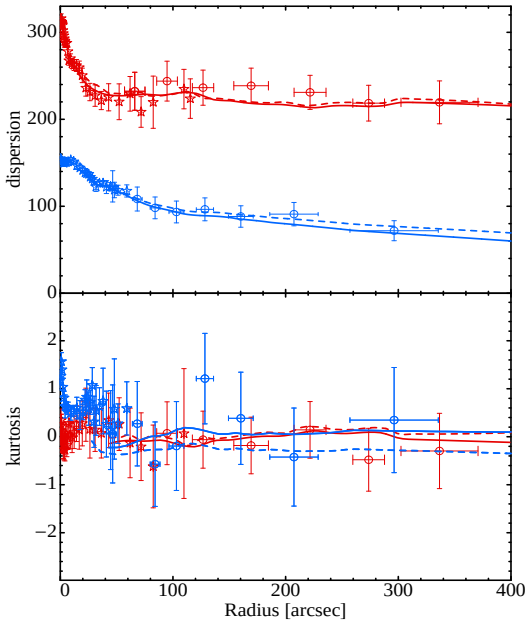

Fig. 2. Dispersion profile (top) and kurtosis (bottom) for the galaxies NGC 4494 (blue) and NGC 4374 (red). Dotted and continuous lines are the isotropic and (radially) anisotropic best model respectively. The anisotropy profile is mainly constrained by the kurtosis fit.

a constant mass-to-light ratio (M/L) galaxy than of DM dominated systems where "flatter" dispersion profiles are generally expected (R+03). On the other hand, orbital anisotropy can also project along the line-of-sight and determine the observed trends, with radial orbits generally producing decreasing profiles (e.g. Dekel et al. 2005). This poses even clearly the question of adopting dynamical analysis with an appropriate treatment of the orbital anisotropy[2], in order to solve the well known mass–anisotropy degeneracy.

An efficient and computationally light way to perform the orbital analysis is the adoption of a dynamical analysis based on Jeans equations including the ordinary 2nd velocity moment (dispersion) and the 4th velocity moment (kurtosis) of the dynamical tracers (Łokas & Mamon 2003). This procedure assumes a stellar spheroid (with stellar density modeled as a Sérsic 1968 profile) embedded in a classical NFW halo. The free parameters of this approach are the stellar M/L_*, the two halo parameters (concentration and virial mass or equivalently the halo density, ρ_s, and radius, r_s, characteristic scales) and the anisotropy, β.

This was implemented for the PN datasets for two galaxies representative of the two dispersion classes: NGC 4494 with a characteristic pseudo-keplerian profile (Napolitano et al. 2009, N+09 hereafter) and NGC 4374 with a flat dispersion curve (Napolitano et al. 2011, N+11) which are compared in Fig. 2.

For the "ordinary" galaxy NGC 4494, the combination of dispersion and kurtosis made possible to break the mass-anisotropy degeneracy and show that this galaxy has a significant radial anisotropy outside $2\,R_e$ ($\beta \sim 0.5$, in agreement with predictions from cosmological simulations). However, the typical halo parameters found for this galaxy (e.g. concentration and virial mass) turned out to be still at odd with the LCDM prediction (if the 1st year measurement of WMAP is considered, WMAP1), i.e. with a very low DM fraction in the central regions ($R < 3\,R_e$) which suggests a low-concentration halos (akin to some spiral studies) or even a cored profile (which turned out to fit the data as well as the NFW, see N+09).

For NGC 4374 the dynamical procedure is improved by including also the adiabatic contraction (AC, e.g. Gnedin et al. 2004, G+04) of the dark matter halo. For this system, the combined modeling of the stellar kinematics of the central (<1.5 R_e) regions and the PN kinematics of the outer halo (~5 R_e) favor a dark halo with an adiabatically contracted NFW profile. This contracted halo has a DM excess in the very central regions which accommodates a lower stellar mass to model the dispersion profile and thus a smaller stellar M/L ratio which turns out to be $M/L_* \sim 5.5$, i.e. compatible with a Kroupa IMF. On the contrary, a non contracted halo also is able to provide a good fit to the data, but with a larger stellar mass-to-light ratio, $M/L_* \sim 6.5$, i.e. closer to a Salpeter IMF. In this case the NFW

[2] This is defined as $\beta \equiv 1 - \sigma_\theta^2/\sigma_r^2$ where σ_θ and σ_r are the spherically-symmetric tangential and radial components of the velocity dispersion ellipsoid, expressed in spherical coordinates.

halo requires a higher concentration ($c_{\rm vir} \sim 9$) and higher virial mass ($\log M_{\rm vir} \sim 13.4 M_\odot$) which is barely consistent with the expected value for WMAP1 cosmology and too high for WMAP5. Thus the AC scheme seems to reconcile together a lighter IMF and the consistency with the ΛCDM, although we have checked that a (cored) logarithmic profile can be still well consistent with the data and a Kroupa IMF (see N+11). Interestingly the orbital anisotropy turned out to be almost isotropic in the outer regions and mildly radially anisotropic within $R_{\rm e}$, which indicates a possible connection of the dichotomic dispersion behavior with the stellar orbital distribution.

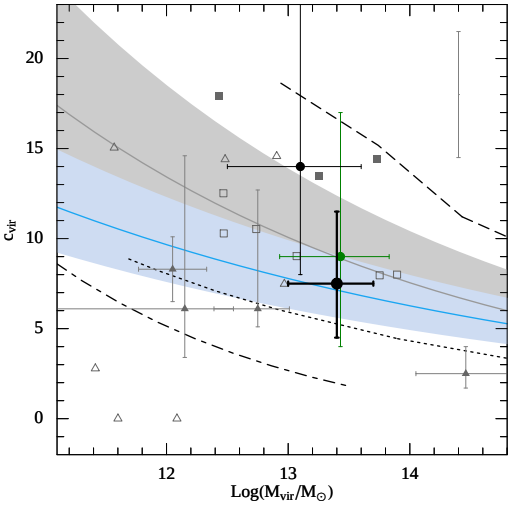

Fig. 3. DM virial mass and concentration. Several reference solutions for NGC 4374 (*large filled circles*) are plotted with other data taken from N+09. The blue and gray shaded regions are the WMAP5 and WMAP1 predictions, respectively. The green small dot with error bars is the "isotropic" solution, the black small dot is "anisotropic" solution (corresponding to a Kroupa IMF), and the big black dot to our favoured anisotropic model with AC. From N+09: *Triangles* and *boxes* mark fast-rotator and slow-rotator ETGs, respectively. The *small filled symbols* mark detailed ETG dynamical results using PNe and GCs (including error bars, where available). The *open symbols* show the dynamics-based ETG results from N+05, with error bars in the upper right corner showing the typical uncertainties. The *dashed line* shows the mean result for X-ray bright groups and clusters, the *dot-dashed curve* is an inference for late-type galaxies, and the *dotted curve* is the trend from weak lensing of all types of galaxies and groups (see N+09 for details).

5. Elliptical galaxies and ΛCDM

At a closer view, the new predictions of the concentration virial mass (cM) relations with WMAP5 cosmological parameters (Macciò et al. 2008, M+08) can solve the controversy of the anomalous concentration-virial mass (cM) distribution of ETGs with respect to the expectations of the ΛCDM, also for the "ordinary" sample. In fact, on the one hand, the lower σ_8=0.75 (WMAP5) implies a lower cM normalization which brings the low concentration halos found in N+09 in agreement with the simulations (M+08). On the other hand, the inclusion of the AC allows halo concentrations which are smaller than the ones obtained without AC, thus moving the too concentrated systems to cM pairs in substantial agreement with the LCDM. This is shown in Fig. 3 where the halo concentration and virial mass of a sample of ETGs are plotted against the predictions of the cosmological simulations in both WMAP1 and WMAP5 parametrization.

Despite the large scatter and few outliers, we now see that generally ETGs are consistent with ΛCDM predictions, although there seems to be some systematic pattern: fast-rotator or ordinary ETGs tend to have lower-concentrations, while slow rotators are more on the high concentration side. With the shift to WMAP5 predictions, the low concentrations become *less* of a problem, and the high concentrations *more*.

This picture might have interesting implications on the formation mechanisms (see e.g. N+11 for a discussion) and needs to be confirmed over a larger sample of galaxies with a detailed dynamics.

6. Conclusions

Detailed dynamics of PN kinematics in ETGs halo regions and the scaling relations of the DM in the central regions are providing new insight on the properties of the DM halos of

these systems. In particular, ETGs seem fairly compatible with predictions of ΛCDM and WMAP5. As seen in Fig. 3, though, their DM halo properties have still a very large scatter which leaves room for alternative density profiles to the typical NFW. If one wants to reconcile the ETG observations with ΛCDM, there are a number of parameters to consider (most of which difficult to control). The most critical is the IMF which acts by changing the DM normalization in the central regions, as well as the adiabatic contraction which is a useful analytical model to reproduce the modification produced by baryons collapse on the DM (unaccounted in the collisionless simulations).

Acknowledgements. I deeply thank A.J. Romanowsky and C. Tortora and the PN.S team.

References

Arnaboldi, M., et al., 1998, ApJ, 507 759
Auger, M. W., et al., 2010, ApJ, 724, 511
Bender, R., et al., 1994, MNRAS, 269, 785
Benson, et al., 2000, MNRAS, 311, 793
Bergond, G., et al., 2006, A&A, 448, 155
Burkert, A. 1995, ApJ, 447, L25
Cappellari, M., et al., 2006, MNRAS, 366, 1126
Chabrier, G. 2001, ApJ, 554, 1274
Ciardullo, R., Jacoby, G. H., & Dejonghe, H. B., 1993, ApJ, 414, 454,
Coccato, L., et al. 2009, MNRAS, 394, 1249
Conroy, C., & Wechsler, R. H. 2009, ApJ, 696, 620
Corsini, E. M., et al., 2008, ApJS, 175, 462
de Blok, W.J.G., Bosma, A., & McGaugh, S., 2003, MNRAS, 340, 657
Dekel, A., et al., 2005, Nat, 437, 707
Douglas, N. G., et al. 2002, PASP, 114, 1234
Douglas, N. G., et al., 2007, ApJ, 664, 257
Emsellem, E., et al., 2007, MNRAS, 379, 401
Fukazawa, Y., et al., 2006, ApJ, 636, 698
Gentile, G., et al., 2004, MNRAS, 351, 903
Gnedin, O. Y., et al., 2004, ApJ, 616, 16
Halliday, C., et al., 2001, MNRAS, 326, 473
Hyde, J. B., & Bernardi, M., 2009, MNRAS, 394, 1978
Humphrey, P. J.,et al., 2006, ApJ, 646, 899
Khochfar, S., & Silk, J. 2006, ApJL, 648, L21
Łokas, E. L., & Mamon, G. A. 2003, MNRAS, 343, 401
Macciò, A. V., Dutton, A. A., & van den Bosch, F. C. 2008, MNRAS, 391, 1940
Merrett, H. R., et al., 2006, MNRAS, 369, 120
Moore, B., et al., 1999, MNRAS, 310, 1147
Napolitano, N. R., Arnaboldi, M., Freeman, K. C., & Capaccioli, M., 2001, A&A, 377, 784
Napolitano, N.R., Arnaboldi, M., & Capaccioli, M., 2002, A&A, 383, 791
Napolitano, N. R., et al. 2005, MNRAS, 357, 691
Napolitano, N. R., et al. 2009, MNRAS, 393, 329
Napolitano, N. R., Romanowsky, A. J., & Tortora, C. 2010, MNRAS, 405, 2351
Napolitano, N. R., et al. 2011, MNRAS, in press (preprint: arXiv:1010.1533) (N+11)
Navarro, J.F., Frenk, C.S., White, S.D., 1997, ApJ, 490, 493 (NFW)
Noordermeer, E., et al., 2008, MNRAS, 384, 943
O'Sullivan , E., & Ponman, T. J., 2004, MNRAS, 349, 535
Paolillo, M., Fabbiano, G., Peres, G., & Kim, D.-W., 2003, ApJ, 586, 850
Pellegrini, S., & Ciotti, L. 2006, MNRAS, 370, 1797
Pellegrini, S., et al., 2007, ApJ, 667, 731
Peng, E. W., Ford, H. C., & Freeman, K. C., 2004, ApJ, 602, 685
Persic, M., Salucci, P., & Stel, F., 1996, MNRAS, 281, 27
Puzia, T. H., et al., 2004, A&A, 415, 123
Richtler, T., et al., 2004, AJ, 127, 2094
Romanowsky, A. J., et al., 2003, Science, 301, 1696
Romanowsky, A. J., et al., 2009, AJ, 137, 4956
Salpeter, E.E. 1955 ApJ, 121, 161
Sersic, J. L. 1968, Atlas de galaxias australes (Cordoba, Argentina: Observatorio Astronomico, 1968)
Statler, T. S., & Smecker-Hane, T., 1999, AJ, 117, 839
Thomas, P. A., & Couchman, H. M. P., 1992, MNRAS, 257, 11
Tortora, C., et al., 2009, MNRAS, 396, 1132
Tortora, C., et al., 2010, ApJL, 721, L1

van den Bosch, F. C., et al., 2007, MNRAS, 376, 841

White, S. D. M., & Rees, M. J. 1978, MNRAS, 183, 341